Experimental Heat-Transfer Studies of Hypervelocity Flight in Planetary Atmospheres

J. S. Gruszczynski* and W. R. Warren Jr.†
General Electric Company, Valley Forge, Pa.

The results of an experimental study of blunt-body heat-transfer problems during entry into planetary atmospheres are presented. Equilibrium gas radiance and convective heat-transfer rates were measured in several CO_2-N_2 gas mixtures over a simulated flight velocity range (approximately) of 30,000 to 45,000 fps. An electrically driven shock tube was used to provide the simulated hypervelocity flight conditions. An unresolved problem concerning the apparent influence of gage surface material on measured convective heat-transfer rates is identified and discussed. The properties and performance of a total radiation cavity gage, used to obtain the gas radiance data, are described. It is shown that species concentrations in a CO_2-N_2 mixture have only a small effect on convective heating rates. A similar conclusion for gas radiance is inferred at flight velocities above 32,000 fps. The experimental results are compared with appropriate theoretical predictions and other experimental data and are used to predict stagnation-point radiative and convective heating for Venus entry trajectories.

Nomenclature

A = area
C_D = drag coefficient
V = voltage
H = altitude
I = radiant intensity
M = Mach number
P = pressure
R_N = nose radius
T = temperature
U = velocity
h = enthalpy
i_g = gage current
l = calorimeter gage thickness
m = mass
$\dot{q}$ = heat-transfer rate
t = time
γ_e = entry angle down from horizontal
λ = wavelength
ρ = density

Subscripts

1 = initial driven tube conditions
2 = behind incident shock
W = wall
R = radiative
c = convective
e = entry conditions (also equilibrium)
f = flight conditions
0 = reference conditions
s = stagnation conditions (also shock)
∞ = freestream conditions

1. Introduction

A VEHICLE entering a planetary atmosphere will be subjected to severe aerothermodynamic conditions similar to those encountered during re-entry into the Earth's atmosphere. A great deal has been learned about Earth re-entry during the past decade so that much of the background knowledge required for the investigation of near planet entry problems now exists. However, certain characteristics of planetary entry are new. The purpose of this paper is to explore the effects of these characteristics on entry vehicle heat transfer through the conduction of a shock tube experimental study.

The framework of the investigation is the simulation of flight into the atmosphere of Venus by a zero-lift ballistic vehicle on a relatively "soft" entry trajectory; that is, the vehicle will decelerate to subsonic velocities at fairly high altitudes and traverse a large portion of the atmosphere at terminal velocities (with or without the aid of additional retardation systems). Such a flight path would be attractive for the conduction of atmospheric property experiments. Our concern, however, is not with the terminal function of such a vehicle but rather with the early entry phase in which the surface heat transfer establishes perhaps the most important design requirement, the weight of the heat-protection system. We have restricted the study to the investigation of the equilibrium radiative and convective heat transfer to the stagnation region of a blunt body and have applied the results to the calculation of stagnation region heat transfer for vehicle parameters corresponding to what might be considered limits on soft trajectories for Venus entry.[1]

Two important characteristics of flight into the atmospheres of the near planets from the point of view of surface heat transfer are the initial entry velocity and the composition of the atmosphere. The escape velocities for Mars and Venus are approximately 16,400 and 34,200 fps, respectively. A vehicle approaching directly from space (no planetary orbit phase) will enter the atmosphere at least at its escape velocity; however, for various mission considerations, such as time of flight, relative position of the planets at entry, and signal transmission capability, it will probably be required to enter the Martian atmosphere in the 20,000- to 25,000-fps range and the Cytherean atmosphere in the 35,000- to 45,000-fps range. Thus, we can restrict our current interest in planetary atmospheric flight to an upper velocity limit of about 45,000 fps. In terms of our Earth reference, this is well into the superorbital or hypervelocity flight regime, a field in which aerothermodynamic research studies have been initiated only in the past few years. A key aspect of this flight regime is the generally increased importance of radiative heat transfer compared to its importance in suborbital flight.

Received September 27, 1963; revision received April 6, 1964. This work was supported in part by the Jet Propulsion Laboratory of NASA under JPL Contract 950297. The authors are indebted to D. A. Rogers and his associates in the Electron Physics Section of the Space Sciences Laboratory for their invaluable contributions to this work.

* Specialist, Hypersonics Research, Space Sciences Laboratory. Member AIAA.

† Manager, Aerothermodynamics Research, Space Sciences Laboratory. Associate Fellow Member AIAA.

Perhaps the clearest distinction between flight in the atmosphere of the Earth and flight in the atmospheres of Mars and Venus is the uncertainty of the composition of the near planets' atmospheres. It might be expected that this could lead to a large uncertainty in surface heat transfer, particularly that due to radiation. Many investigators believe that the atmospheres of interest are composed of a mixture of molecular nitrogen and carbon dioxide with trace amounts of water vapor and other "contaminants." The major part of the work reported here has used the assumed Cytherean atmosphere—composition and temperature, density, and pressure profiles—shown in Fig. 1.[1] We have used analytical results and some experimental data to infer the effects of composition on the results obtained in the nominal mixture caused by varying the concentration of the two major constituents.

The stagnation region heat transfer is composed of boundary-layer (convective) heating and radiative heating from the shock-layer gases. The radiative heat transfer can be thought of as coming from two sources: equilibrium radiation from the parts of the shock layer which have reached thermodynamic and chemical equilibrium, and nonequilibrium radiation from the parts of the shock wave and shock layer in which the gas has not had time to distribute its kinetic energy among its various degrees of freedom. Nonequilibrium radiative heat-transfer data are not presented in this paper; however, the potential importance of this mechanism is discussed qualitatively in a later section of the paper.

Figure 1 also presents an altitude-velocity flight map for the assumed atmosphere. Shown on this figure are equilibrium thermodynamic properties in a blunt-body stagnation region over a wide range of flight conditions. Lines of equilibrium radiation intensity for the stagnation region conditions are also given. These radiances were calculated by summing the radiation from specific de-excitation mechanisms,[2] the contribution of each being determined by the equilibrium composition of the gas.[3] The method of calculation includes the effects of self-absorption over a 1-cm length. The reader is referred to Ref. 4 for the analytical and computational details used in the prediction of radiant intensity. Two typical entry vehicle trajectories are also shown in Fig. 1. It can be seen that deep atmospheric penetration and entry at high velocities produce severe radiation environments.

Measurements of convective heat transfer and gas radiance were made in an electrically driven shock tube; this facility is ideally suited to this type of study, since its flight simulation capabilities extend well into the superorbital regime. The experimental results have been compared to appropriate theoretical predictions. A brief description of the shock tube and its performance characteristics is presented in the next section. (See Refs. 5 and 6 for detailed discussions of the properties of electrically driven shock tubes.)

2. Experimental Techniques

Description of Shock Tube

The electrically driven shock tube used in this study (a larger version of the tube described in Ref. 5) is illustrated in Fig. 2. A high-temperature, high-pressure, low-molecular-weight driver gas is produced by a rapid axial discharge of electrical energy stored in a capacitor bank into a helium-filled driver. After the energy is distributed through the driver gas, the diaphragm ruptures, and a strong shock wave is generated in the low-pressure, driven tube gas. The driver dimensions shown in Fig. 2 are maximum values; for this study, the driver was shortened by the insertion of plastic cylinders to a length of either 18 or 30 in.

Several test flows are available in a shock tube: the flow behind the incident shock wave, the stagnated reflected region gas, and the flow in the shock layer of a model located in the flow behind the incident wave. The latter test flow

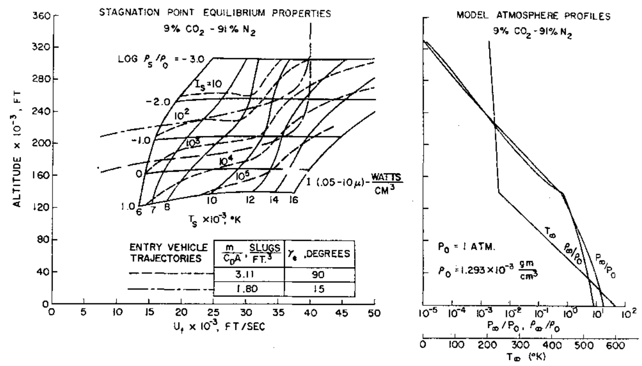

Fig. 1 Blunt-body stagnation-point equilibrium gas properties and atmospheric model assumed for Venus.

has been used for both the convective and radiative studies reported here.

Shock Tube Properties

Using thermochemical equilibrium properties for a 9% CO_2-91% N_2 mixture,[3] calculations of thermodynamic properties and species concentrations in the test regions of interest in the shock tube have been made. Figures 3 and 4 present some of these results. Also shown are the simulated flight velocities for the model test flow which are essentially a function only of the incident shock wave velocity for the range of conditions treated. Comparison of these figures with the altitude-flight velocity map of Fig. 1 shows the flight velocity simulation achieved at specific shock tube conditions.

Shock Tube Performance

Since electrical shock tube performance capabilities in terms of flight simulation are discussed in some detail in Ref. 5, only performance data pertinent to the present experimental results will be discussed here.

The shock speed was obtained by observing the luminous profile of the shock wave with collimated photomultipliers as it passes five stations ahead of the model station. The signals from each photosensor were differentiated and added to a raster signal displayed on an oscilloscope. The arrival of the shock front at each station can be read with an accuracy of ± 0.5 μsec which, for example, over a 2-ft interval at 30,000 fps, gives shock speed with an accuracy of better than 1%. The wall pressure history behind the incident shock was also monitored at several stations for the purposes of 1) obtaining additional shock velocity data, 2) verifying the equilibrium predictions, and 3) insuring that the reflected

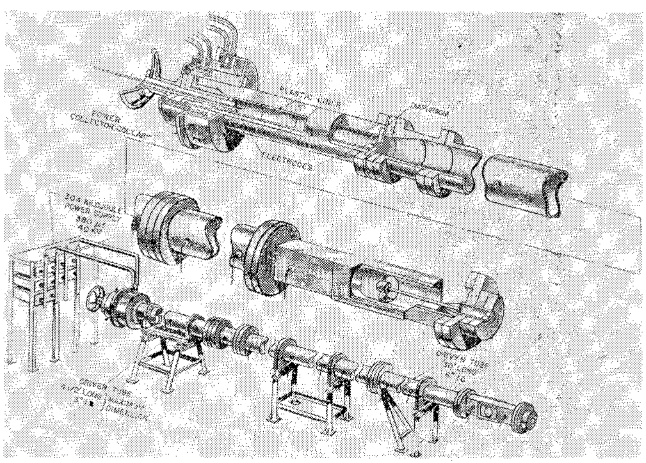

Fig. 2 Hypervelocity shock tube with electrically heated helium driver.

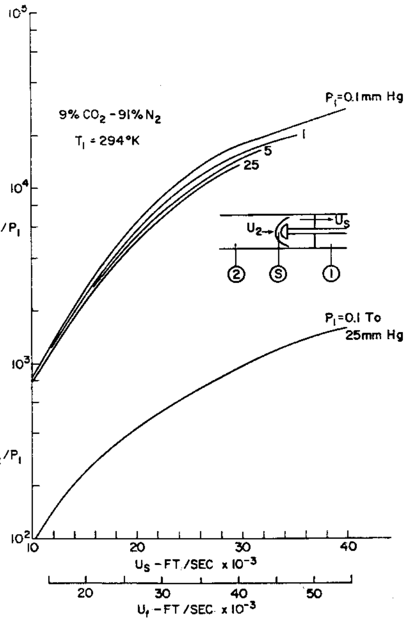

Fig. 3 Pressure behind incident shock wave and at model stagnation point in the shock tube: equilibrium gas properties.

expansion wave from the driver does not interfere with the test gas flow.

Photometric and spectrographic methods were used to obtain information on the quality of the test flows. The emitted light from the gas behind the incident shock wave was monitored with a multichannel monochromator. Figure 5 shows oscilloscope traces obtained at three different wavelengths. Note the fairly narrow bandpass of each channel. In general, the arrival of the shock front is followed 1) by a short duration (order of 1 μsec) pulse of high-intensity radiation, caused by nonequilibrium effects, 2) a period of constant radiation from the equilibrium driven gas, and 3) a period of nonsteady radiative intensity from the driver-driven gas mixture in the contact front. From such data, the steadiness and duration of the driven gas approaching the model upstream of the model bow shock wave was determined. A two-color photometer, with its entrance slit focused on a point slightly ahead of the model stagnation point, was used to observe the shock layer luminosity history for each run. Oscilloscope traces of the signal from this instrument are shown in Fig. 6. In addition to its usefulness in determining the test flow duration and the steadiness, data of this type also provide a measure of the steady-state

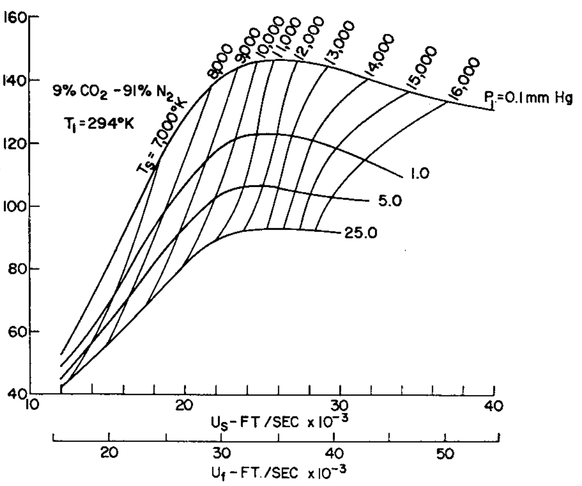

Fig. 4 Density and temperature at model stagnation point in the shock tube: equilibrium gas properties.

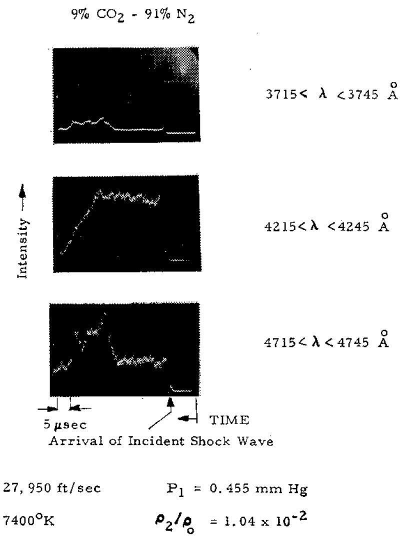

Fig. 5 Oscilloscope traces of radiation behind incident shock wave.

model flow establishment time. It is interesting to note that the blue signal sometimes shows an increase of intensity upon the arrival of the contact front, whereas the red channel always indicates a drop in radiation at this time. The duration of the test flows obtained in this manner agrees closely with other measurements.

Several procedures were used to insure that the contamination of the test gas was at a minimum for each test. Before each run, the driven tube, which had a measured leak rate of less than 0.8 μ Hg/min, was carefully cleaned and pumped for several hours at approximately 8 μ Hg. In addition, the

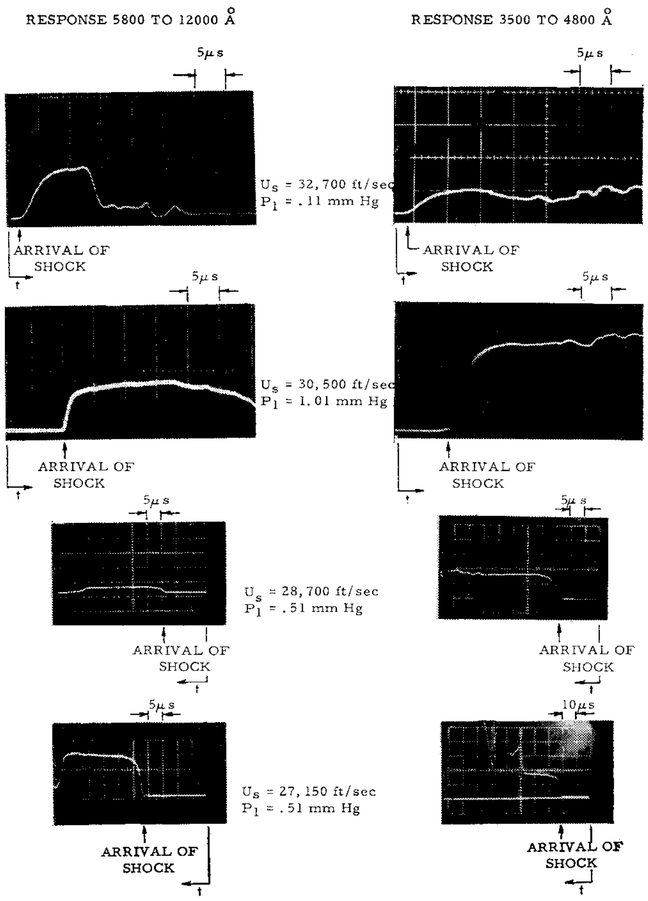

Fig. 6 Oscilloscope traces showing responses of the red and blue sidewall photomultipliers viewing model shock layer.

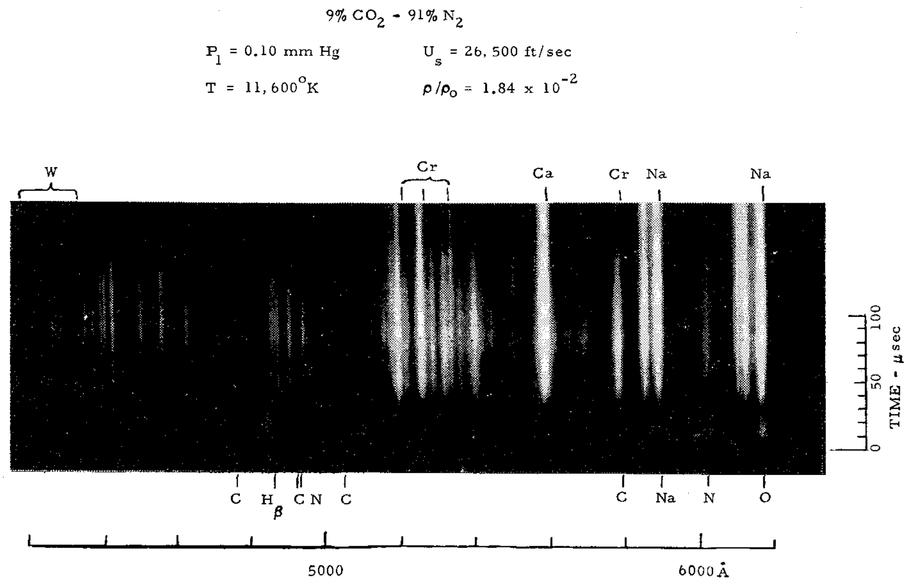

Fig. 7 Time resolved spectrogram of gas in the stagnation region of hemispherical model. Instrument has f/3.5 glass optics and time resolution of 11 μsec.

pure premixed gas was cold-trapped and flushed through the tube at the test pressure for about 30 min prior to a run. A time resolved spectrogram of the stagnation region flow observed through a slit in the sidewall of the shock tube is shown in Fig. 7. The spectrum shows that the test flow (approximately 0 to 20 μsec) is largely contaminant free; that is, the strong line radiation following the available test time generally does not extend into the test gas. Although there is the possibility that small quantities of easily ionized contaminants exist in the test gas, the high stagnation region ionization levels associated with the hypervelocity regime are such that the number of electrons contributed by the contaminants should be negligible. Note the prominent H_β line in the test flow. The analysis of the spectra indicates that a small fraction of water vapor in the test gas (order of 10 ppm) would be sufficient to produce the observed line intensity. Although this amount of hydrogen should not appreciably influence the thermochemical properties of the gas in the stagnation region, its presence in the spectrum allows the calculation of electron concentration by the application of Griem's analysis of the Stark broadening effect.[7] Such calculations have been made by Sadjian[8] for several test spectra; his results indicate that the ion concentration of the test gas agrees within a factor of two with the concentrations predicted by the thermochemical equilibrium calculations[3] in the temperature range of 11,000° to 14,500°K.

3. Stagnation-Point Convective Heat Transfer

For some time, a controversy has centered about the subject of convective heat transfer in the hypervelocity flight regime because of a disagreement between data obtained by the second author of this paper[5] and those of several other investigators. This disagreement has been summarized by Rose and Stankevics in a recent paper.[9] For this reason, convective heat-transfer measurement techniques for the blunt model test configuration in the shock tube were investigated in some detail in the present work. Since we have found that the type of gage material used appreciably affects the apparent heat-transfer response of a calorimeter gage, several materials were studied. The thin-film gage technique was also used, since, as a basically different means for the measurement of surface heat transfer, it offered a capability for discrimination between the results obtained for the different materials studied with the calorimeter gage.

A two-calorimeter gage model was used to obtain simultaneous data with gages of different materials or of different geometries. Because of the high heating rates and short test times associated with hypervelocity flight simulation in the shock tube, the use of a gage response in which the heat is assumed to be distributed uniformly through the gage will be in error.[10] Time-dependent temperature distributions and corrections for the uniform heat distribution assumption have been calculated for two types of gage materials [platinum and Hytemco (a nickel-iron alloy)] and for several different gage thicknesses. The correction curves are shown in Fig. 8. The relatively large correction for the thick Hytemco gage is caused by the fact that the heat is conducted slowly into this material in comparison with the platinum material, thereby producing steep temperature gradients close to the heated surface. Corrections for the temperature distribution in thinner gages of higher conductivity material are small, but such a gage may lose some heat to its backing material early in the test time. Considerations of this type lead to the choice of gage thickness. For example, we have concluded that, for the test parameters encountered in this work, a 0.002-in. thickness was most appropriate for platinum gages.

Hytemco gages were used to obtain data reported in Ref. 5, whereas the data of other investigators[9,11,16] were taken with platinum gages. Figure 9 shows traces taken during a shock tube test from both the platinum and Hytemco gages in a

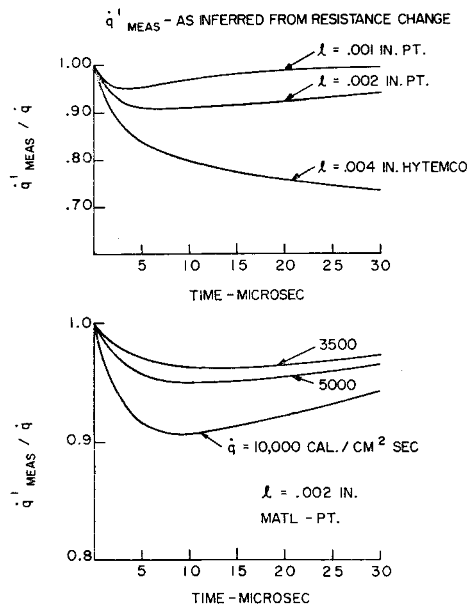

Fig. 8 Theoretical corrections for platinum and Hytemco calorimeter heat-transfer gages for various thicknesses and heating rates. Correction only for temperature distribution effect and not for losses to backing material.

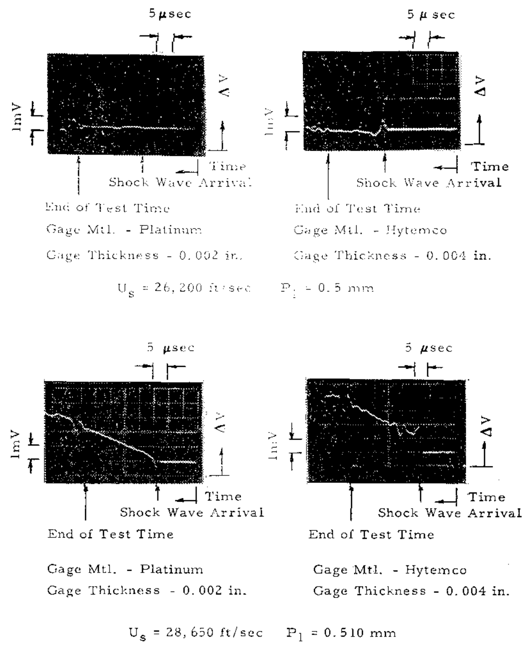

Fig. 9 Typical calorimeter gage responses in two-gage model test: upper traces, zero gage current applied; lower traces, normal gage current applied.

two-gage model. It has been reported by Rose and Stankevics[9] that a spurious signal was observed with a gage thickness corresponding to that of the present Hytemco gage when no battery current was flowing. Figure 9 indicates that this effect is absent in the present data. However, there is significantly more signal noise generated in the Hytemco gage during the establishment of the test flow. The second gage evaluation test was the measurement of convective heat transfer (normal gage current) using the two-gage model. Results of this type are shown in Fig. 9. Again, the more pronounced noise associated with the Hytemco gage signal is seen; nevertheless, a significant period of test time exists during which accurate slope measurements of the Hytemco signal can be made. The platinum gage signal is quite clean throughout the major portion of the test time.

The reduced heat-transfer data for these two gage materials have been found to differ significantly; the Hytemco gage usually gave an apparent heat-transfer rate of about twice the value obtained with the platinum gage. Also, more scatter is found in the Hytemco gage data. Since it was not apparent which material gave the correct signal, or indeed, if either material did so, we investigated two other approaches to the measurement of stagnation-point heating. First, to determine if the Hytemco alloying process had a significant effect, nickel calorimeter gages were constructed and run. However, the nickel results tended to agree with the Hytemco data. Second, heat-transfer measurements were made using the thin-film gage technique. The test response of such a gage is shown in Fig. 10. The reduced heat-transfer rates, corrected for surface material temperature change,[12] are shown in Fig. 11 along with the observed platinum, Hytemco, and nickel calorimeter gage data. Data for air, as well as for the 9% CO_2-91% N_2 mixture, are shown. From this figure, it is seen that the platinum thin-film results are at the general level of the platinum calorimeter heat-transfer data. We have also included in Fig. 11 the recently published data of Compton and Chapman at a flight velocity simulation level of about 36,000 fps[13] which were obtained from observations of the time required to initiate melting of free-flying aluminum models. These data support the level of the platinum calorimeter gage measurements. Measurements of other investigators using calorimeter gages in a shock tube are not shown, since they generally agree with the present data using the same technique.

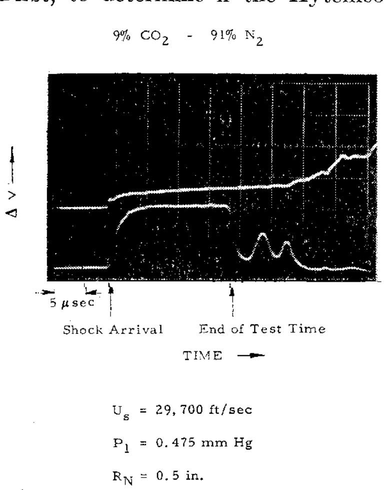

Fig. 10 Response of stagnation-point thin-film heat-transfer gage: upper trace, heat-transfer gage; lower trace, sidewall photomultiplier viewing shock layer ahead of the stagnation point.

We have interpreted and used the information given in Fig. 11 as follows. Three techniques for the measurement of hypervelocity stagnation-point heat transfer [platinum calorimeter gage (shock tube), platinum thin-film gage (shock tube), and melting aluminum model (range-type facility)] tend to agree in the vicinity of a simulated flight velocity of 36,000 fps. The level of heating given by these methods disagrees with the level obtained with Hytemco and nickel calorimeter gages. It is possible that this difference is caused by a combination of boundary-layer electronic nonequilibrium and gage surface catalysis effects. An approximate treatment of electron recombination in a shock tube model boundary layer is given by Rose and Stankevics,[9] and recent work on catalytic effects for materials similar to those of interest have been reported by Myerson[14] and Hartunian.[15] These references do not rule out the nonequilibrium-catalytic explanation of the present results; however, basic work in these areas has not yet progressed to the point that we can conclude that this explanation is justified. Also, there is not yet a sufficient quantity of shock tube data in the hypervelocity regime with gage surfaces other than platinum to provide valid statistical arguments for or against the suggested combined effect. Because of the existence of two other sets of hypervelocity data taken with platinum calorimeter gages in gases of interest in a planetary entry study,[9, 16] we have used the present data obtained with platinum gages in the subsequent discussions of convective heat-transfer results. However, the possibility that surface heat transfer, under hypervelocity flight conditions at relatively high gas densities, can be significantly influenced by

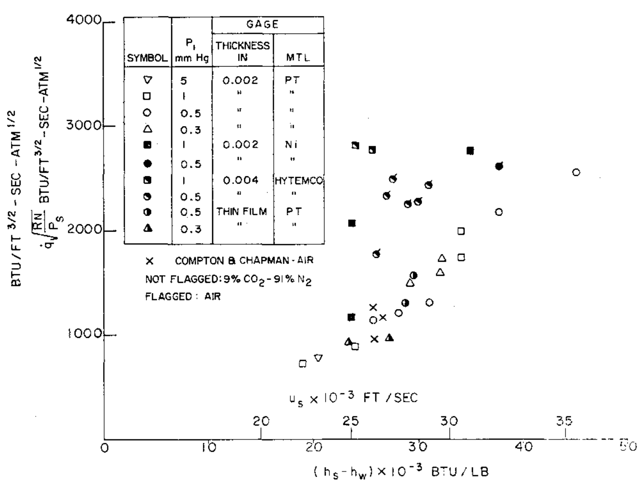

Fig. 11 Comparison of stagnation-point heat-transfer results obtained with different material gages.

surface material properties must not be discounted without additional study.

The convective heat-transfer data obtained with platinum calorimeter and thin-film gages are presented in Fig. 12. The composition in which most of the present data were obtained was 9% CO_2 and 91% N_2. A few data were also obtained in a mixture containing 87% CO_2 and 13% N_2. Most of the data were taken with 0.002-in.-thick platinum calorimeter gages. A new gage was used for each test run. A 0.5-in. nose radius hemispherical model was used for all data shown in Fig. 12. As described earlier, a correction factor was applied to the observed calorimeter gage response to take into account the nonlinear temperature distribution across the thickness of the gage element (Fig. 8), and the thin-film gage data were adjusted for the variation of the backing material properties due to a change in its temperature during the test time.[12]

In analyzing the data, the possible contribution of radiative heating to the measured heat-transfer rates was considered. For enthalpy levels corresponding to flight velocities below 37,000 fps and stagnation-point densities of the present experiments, the radiative flux from the shock layer to the gage was estimated using data of Ref. 2 and found to be less than 10% of the measured heat-transfer rate. However, for higher enthalpies, the radiation becomes larger and may add considerably to the measured rates. The amount of incident radiation which the gage will absorb depends on the surface reflectivity, which itself is a function of the wavelength and the surface conditions. Since these factors are difficult to evaluate for each gage, it was assumed that the gage surface will absorb 50% of the incident radiant energy. Appropriate corrections were made and the data plotted showing a range of uncertainty (25 to 75% absorption) due to the radiative heating contribution.

The present platinum gage data are compared in Fig. 12 with the theoretical solutions of Hoshizaki for stagnation-point laminar boundary-layer heat transfer in CO_2 and in air.[11] The agreement between experiment and theory is reasonably good over the range of data; however, there is tendency for the data to favor the air prediction at the lower simulated flight velocities and the CO_2 prediction at the higher velocities.

All experimental data available to the authors on convective heat transfer in N_2, CO_2, or N_2-CO_2 mixtures are shown in Fig. 13 together with the theoretical predictions of Hoshizaki. The data in CO_2 include the free-flight measurements of Yee, et al.[17] and the results of shock tube experiments by Rutowski and Chan[18] which were taken at relatively low stagnation enthalpies and, thus, provide results at velocity levels lower than that of the present investigation. In the simulated velocity range between 30,000 and 38,000 fps, it can be seen that the heat-transfer results in the 9% CO_2-91% N_2 gas mixture tend to lie below the CO_2 shock tube

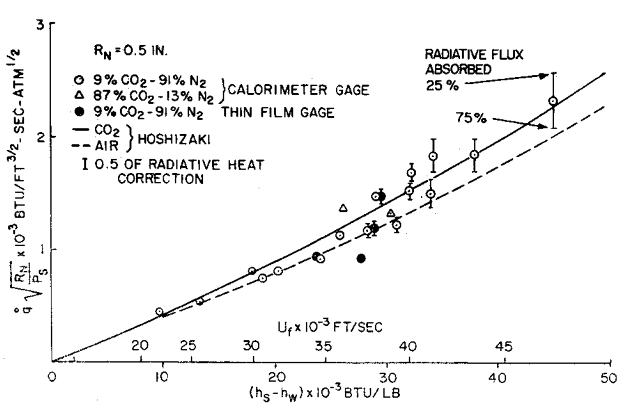

Fig. 12 Hypervelocity stagnation-point heat transfer in simulated planetary atmospheres.

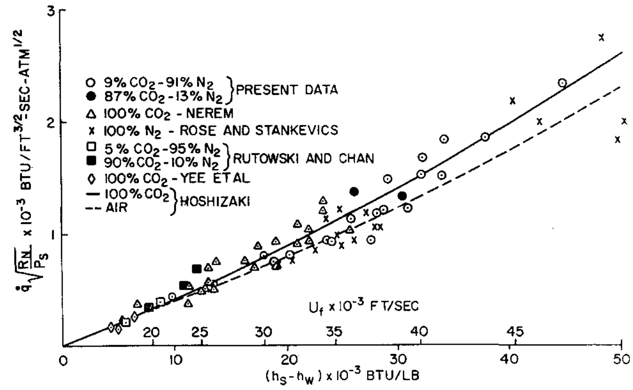

Fig. 13 Comparison of stagnation-point heat-transfer results in carbon dioxide, carbon dioxide-nitrogen mixtures, and nitrogen.

data of Nerem[16] and in general agreement with the N_2 results of Rose and Stankevics.[9] Therefore, both the theoretical and experimental information given in Fig. 13 support the existence of a somewhat higher level of heat transfer in the CO_2-rich mixtures over that in the N_2-rich mixtures in the hypervelocity flight regime.

4. Radiation Study

We have used the stagnation region flow in front of a hemispherical model for the measurement of gas radiance properties. It has several advantages in this application. First, the flow establishes rapidly and remains relatively steady during the test time, in contrast, for example, with the somewhat unsteady flows in the reflected region of a shock tube. Second, by sensing radiative fluxes through the model, interference from the unsteady and fairly thick sidewall boundary layer that develops in the tube after the passage of the incident shock wave is eliminated. Third, by using a collimating sensing system at the stagnation region, the radiating gas sample of interest has essentially uniform properties, and its dimensions can be accurately measured. Fourth, the flow is steady in the laboratory coordinates so that the requirements on time response of the instrumentation used are not overly severe. One major disadvantage of this test configuration is that the freestream flow (the flow behind the incident wave) is highly excited thermochemically compared to the freestream flow a vehicle will experience in flight through an atmosphere. However, if we restrict the study to equilibrium radiation, this test configuration provides a good simulation of the stagnation region in hypervelocity flight.

The radiation intensity of a column of gas normal to the model surface at the stagnation region between the surface and the bow shock wave has been measured by a new cavity gage technique described below. Sidewall observations of the bow shock wave region have included the time resolved spectroscopic observation of the stagnation region and the measurement of bow shock wave standoff distance through the use of collimated phototubes. Concerning this latter measurement, it was found that the standoff distance during the test time was in good agreement with the predictions of Serbin[19] for several test conditions. Thus, his predictions were used for establishing the radiative column length required for the reduction of the cavity gage data.

The total radiation cavity heat-transfer gage is sketched in Fig. 14. This gage consists of a cylindrical cavity, the inside of which is coated with a thin-film heat-transfer gage as shown schematically in the figure. Its advantage is the coupling of a fast response time (the order of tenths of microseconds) with the ability to keep difficult-to-determine material surface properties from interfering with the response of the gage. The gage can be used for various types of shock

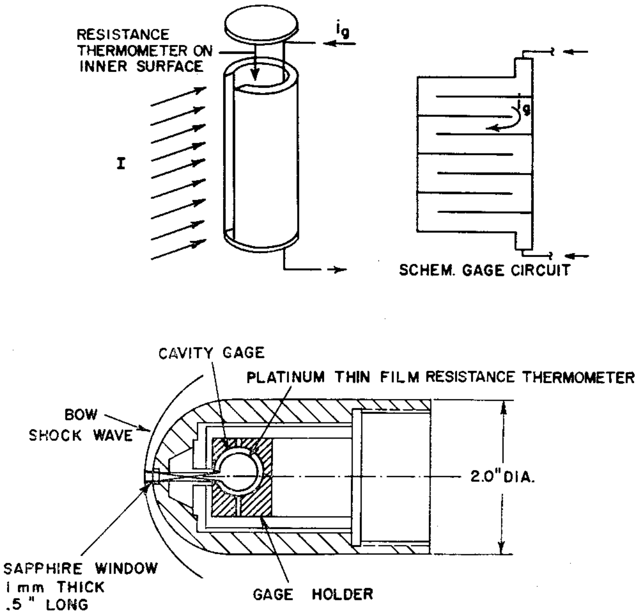

Fig. 14 Sketch of cavity gage concept and gage model configuration used for present measurements: 2-in.-diam. model shown.

tube radiation measurements.[20] In the present study, we have used it only in the configuration shown in Fig. 14 in which a sapphire window was located at the stagnation region of the model. Therefore, this gage system is collimated and senses only the radiation from a region of shock layer gas close to the axis of the model. Since, for the test conditions of interest here, the stagnation region gas has almost uniform temperature and density and is essentially transparent, the signal can be interpreted in terms of the radiance of the stagnant gas. Oscilloscope traces of the cavity gage signal are shown in Fig. 15. The approximately parabolic signal is typical of the response of a thin-film gage to an approximately steady heating rate. Traces from the red phototube sidewall observation of the shock layer, which indicate the establishment, duration, and steadiness of the test flow, as discussed earlier, are also shown in Fig. 15. The history of stagnation gas radiance, as determined by analysis of one of the thin-film traces in Fig. 15, is shown in Fig. 16.

Cavity gage measurements of the total radiative intensity of the stagnation region gas are presented in Fig. 17. Results have been obtained for shock velocity values between 22,000 and 34,000 fps. Also shown on Fig. 17 are the theoretical curves (based on the predictions of Ref. 2 for the 0.2-to 10-μ spectral region) for the shock tube property ranges covered by the experimental conditions. The radiance has been normalized by the stagnation region density ratio to the 1.55 power which brings the theoretical curves into reasonably good agreement over the property range of interest. In general, the experimental points scatter near the theoretical predictions. There is a tendency for the experimental results to be higher than theory at shock velocities below about 28,000 fps. Above this value, the points generally group somewhat below the predicted level. Note the few points corresponding to P_1 values of 0.1 mm Hg. These lie significantly above the level predicted by the equilibrium theory and the general level of the experimental data at higher pressures. We associated this behavior with the initiation of nonequilibrium effects in the shock layer. Radiation from a nonequilibrium air shock layer has been investigated experimentally by Page.[21] Since the nonequilibrium process in the model test configuration will be different from that investigated by Page because of the high temperature and dissociation level of the gas entering the shock layer in the shock tube, a direct comparison with his results is not necessarily valid. However, it is observed that the values of the few low pressure points are compatible with those presented by Page.

Two points from different test gas mixtures are also shown in Fig. 17. Although more data are required for the study of the importance of gas composition, there is reasonable agreement between these points and the other information shown. As discussed below, this is the expected result.

5. Application of Results

The radiance and convective heat-transfer results described previously have been used to predict the stagnation-point heating for blunt vehicles corresponding to the trajectories shown in Fig. 1. The theoretical data of Ref. 2 (0.05 to 10 μ), with an experimentally suggested correction distribution (40% increase at 36,000 fps decreasing linearly to 0% at 30,000 and 40,000 fps), were used for the radiative properties. The theory-experiment comparison in Fig. 17 supports the validity of this assumption. Hoshizaki's theoretical curve for CO_2 was used for the convective heat-transfer rates. The resultant heat flux histories are shown in Fig. 18.

The high m/C_DA, 90° entry angle trajectory exhibits a severe radiation heating load with a peak rate about five times that of the peak convective heating rate for a 1-ft radius body. For the lower mass, lower angle trajectory, the heating rates are more moderate with the convective mechanism replacing the radiative in maximum severity. Note point A marked on both radiative curves in Fig. 18. It can be shown from Fig. 1 and Ref. 2 that it is only after this point that strong differences in radiation between CO_2-N_2 mixtures of widely varying compositions (and air) due to CO

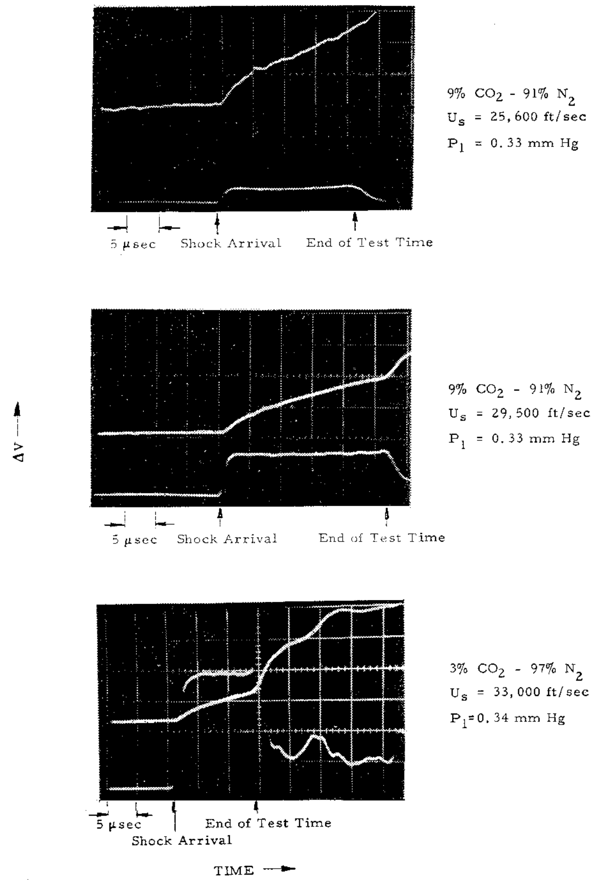

Fig. 15 Oscilloscope trace showing thin-film cavity gage response during test gas flow: upper trace, model stagnation region gavity gage; lower trace, sidewall photomultiplier sensitive in the red viewing stagnation region shock layer.

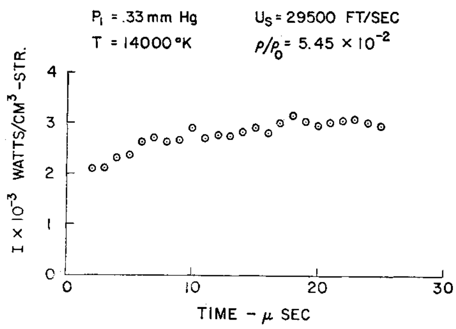

Fig. 16 Radiance of model stagnation region gas as a function of time after arrival of incident shock wave at model. Data obtained from analysis of thin-film cavity gage signal shown in Fig. 15.

and CN band radiation become apparent. This is reflected in the shape of the radiative pulses after point A and in the low velocity leveling of the theoretical curves in Fig. 17. Above a simulated flight velocity of about 32,000 fps, Ref. 2 shows that the gas radiance from these mixtures is dominated by the free-free interactions and deionization of nitrogen, oxygen, and carbon ions and is essentially dependent only on enthalpy and density levels (or flight velocity and altitude). Thus, for initial entry velocities of the order of 40,000 fps or more, where the radiative heating peaks above 35,000 fps, the complexity of the equilibrium radiation problem caused by our lack of knowledge of gas composition may be considerably reduced.

Nonequilibrium radiation contributions are not included in the curves of Fig. 18. If this mechanism for planetary gases gives levels similar to those found by Page[21] for air (order of 20 Btu/ft^2-sec at 36,000 fps), the nonequilibrium radiation will be negligible for trajectories of the type shown.

6. Concluding Remarks

Several planetary entry heat-transfer problems that have not yet been satisfactorily explored can be identified. First,

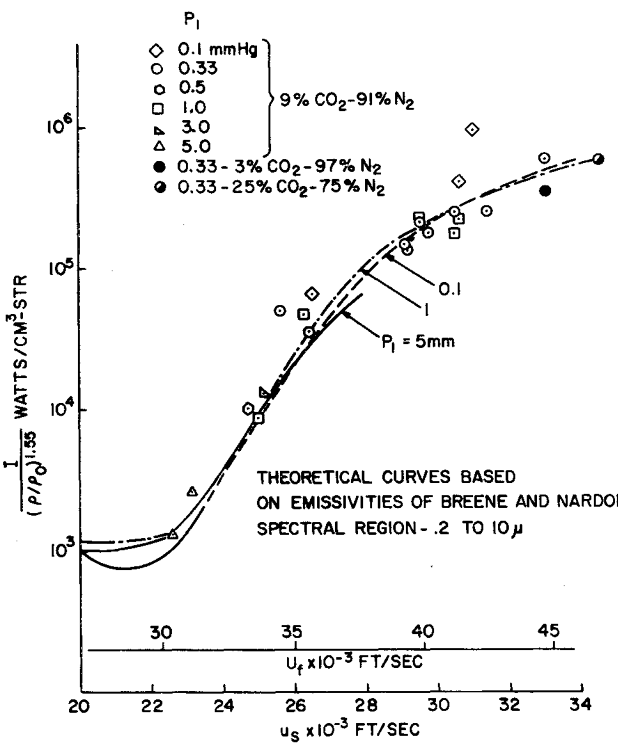

Fig. 17 Stagnation-point radiation in simulated Venusian atmosphere: experimental results obtained with the cavity gage compared to the theoretical predictions.

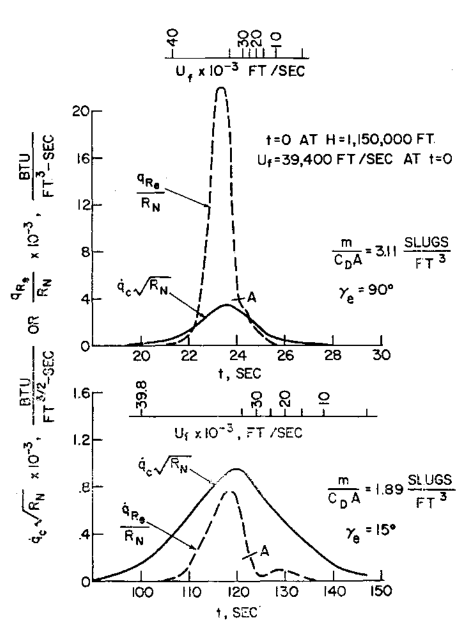

Fig. 18 Radiative and convective stagnation-point heat-transfer rates for atmosphere and entry vehicle trajectories shown in Fig. 1.

an explanation for the apparent gage surface materials effect on convective heat transfer must be found. Second, the validity of equilibrium radiation predictions has not been tested experimentally either in the lower flight velocity ranges or over the range of possible major constituent concentrations (including species other than CO_2 and N_2). Third, the importance of nonequilibrium radiation for the gas mixtures of interest has not been determined. Fourth, the effects of self-absorption and coupled radiative and convective energy fluxes, possibly important for entry at higher velocities than those discussed here, have not been studied. These problems should be the subject of future research in this area.‡

References

1 "Venus-Mars capsule study," General Electric Co. Final Rept., Jet Propulsion Lab. Contract 950250 (July 1962).

2 Breene, R. G., Jr. and Nardone, M. C., "Radiant emission in the atmospheres of the terrestrial planets," *Symposium on Dynamics of Manned Lifting Planetary Entry* (John Wiley and Sons, Inc., New York, 1963), pp. 331–341; also private communication (February 1963).

3 Browne, W. G., Re-Entry Systems Dept., General Electric Co., private communication (June 1962).

4 Nardone, M. C., Breene, R. G., Zeldin, S. S., and Riethof, T. R., "Radiance of species in high temperature air," General Electric Missile and Space Div. Doc. R63SD3 (June 1963).

5 Warren, W. R., Rogers, D. A., and Harris, C. J., "The development of an electrically heated shock driven test facility," 2nd Symposium on Hypervelocity Techniques, Univ. of Denver, Denver, Colo. (March 1962); also General Electric Missile and Space Div. Doc. R62SD37 (April 1962).

6 Camm, J., "Escape velocity shock tube with arc heated driver," 2nd Symposium on Hypervelocity Techniques, Univ. of Denver, Denver, Colo. (March 1962).

7 Griem, H. R., Kolb, A. C., and Shen, K. Y., "Stark broadening of hydrogen lines in plasma," Naval Research Lab. Rept. 5455 (March 1960).

8 Sadjian, H., Space Sciences Lab., General Electric Co., private communication (July 1963).

‡ In a recent paper,[22] James has presented gas radiance data for a range of CO_2-N_2 mixture ratios to a flight velocity of 27,100 fps. Also, the problems of low velocity entry and nonequilibrium radiation have been treated in Ref. 23.

[9] Rose, P. H. and Stankevics, J. O., "Stagnation point heat transfer measurements in partially ionized air," IAS Paper 63-61 (January 1963).

[10] Rose, P. H., "Development of the calorimeter heat transfer gage for use in shock tubes," Rev. Sci. Instr. **29**, 557–564 (1958).

[11] Hoshizaki, H., "Heat transfer in planetary atmospheres at super-satellite speeds," ARS J. **32**, 1544–1552 (1962).

[12] Hartunian, R. A. and Varwig, R. L., "A correction to the thin film heat transfer measurements," Aerospace Corp. Rept. TDR-594 (1217-01) TN-2 (May 1961).

[13] Compton, D. L. and Chapman, G. T., "Two new free-flight methods for obtaining convective heat transfer data," *AIAA Aerodynamic Testing Conference* (American Institute of Aeronautics and Astronautics, New York, 1964), pp. 115–128.

[14] Myerson, A. L., "Interim report on transient heat transfer measurements of catalytic recombination in a step-function flow of atomic oxygen," Cornell Aeronautical Lab. Rept. AF-1412-A-2 (August 1962).

[15] Hartunian, R. A. and Thompson, W. P., "Non-equilibrium stagnation point heat transfer including surface catalysis," AIAA Preprint 63-464 (August 1963).

[16] Nerem, R. M., Morgan, C. J., and Graber, B. C., "Hypervelocity stagnation point heat transfer in a carbon dioxide atmosphere," AIAA J. **9**, 2173–2175 (1963).

[17] Yee, L., Bailey, H. E., and Woodward, H. T., "Ballistic range measurements of stagnation point heat transfer in air and in carbon dioxide at velocities up to 18,000 feet per second," NASA TN D-777 (1961).

[18] Rutowski, R. W. and Chan, K. K., "Shock tube experiments simulating entry into planetary atmospheres," Lockheed Missiles and Space Co., LMSD-288139 (January 1960).

[19] Serbin, H., "Supersonic flow around blunt bodies," J. Aerospace Sci. **25**, 58–59 (1958).

[20] Gruszczynski, J. S., Harris, C. J., Rogers, D. A., and Warren, W. R., "Fast response total radiation gage for measurement of radiant emission from high temperature gas," Institute of Electrical and Electronics Engineers Paper CP 63-438 (January 1963); also General Electric Missile and Space Div. Doc. R63SD11 (January 1963).

[21] Page, W. A., "Shock layer radiation of blunt bodies traveling at lunar return entry velocities," IAS Paper 63-41 (January 1963).

[22] James, C. S., "Experimental study of radiative transport from hot gases simulating in composition the atmospheres of mars and venus," AIAA Preprint 63-455 (August 1963).

[23] Gruszczynski, J. S. and Warren, W. R., "Hypervelocity heat transfer studies in simulated planetary atmospheres," General Electric Co. Interim Rept., Jet Propulsion Lab. Contract 950297 (March 1964).

SEPTEMBER 1964 AIAA JOURNAL VOL. 2, NO. 9

Statistical Behavior of a Turbulent Multicomponent Mixture with First-Order Reactions

Yih-Ho Pao*

Boeing Scientific Research Laboratories, Seattle, Wash.

The dilute turbulent concentration fields of a multicomponent mixture with any type isothermal first-order reaction are investigated. For certain given initial conditions, the reacting concentration fields are related to the nonreacting case provided that the diffusivities of all species with respect to the main solution are equal. This enables us to utilize some known results of turbulent mixing to estimate the rate of decay and/or growth of the reacting turbulent concentration fields. For the case of stationary turbulence with first-order reactions and with *nonequal* diffusivities, where the Reynolds number and Péclet number are large, the small-scale structure of the turbulent concentration fields are investigated under the assumption of local isotropy and local homogeneity. A unified concept for spectral transfer at large wave numbers is proposed which, in essence, is a generalization of the Onsager-Corrsin spectral transfer concept. With this unified spectral transfer concept, as well as other concepts, the reacting concentration spectrum functions are deduced for three wave number ranges: 1) the inertial-convective range, 2) the viscous-convective and viscous-diffusive range for large Schmidt numbers, and 3) the inertial-diffusive range for small Schmidt numbers.

1. Introduction

THE complexities of turbulence have long been revealed, but are far from being completely understood. Despite continuous efforts, it still defies a thorough theoretical treatment, and reliable turbulence measurements are tedious and hard to obtain. The difficulties are mainly due to its randomness, nonlinearity, and inherent three-dimensionality. With the added complexity of chemical reaction in turbulent flow, the problem becomes even more intractable. Fortunately, there are some partial theories, well supported by observations and experimental results, which enable us to understand the phenomena of turbulence and turbulent mixing to a certain extent. Based on these, some problems of turbulent mixing with chemical reaction can be investigated. For an exploratory account of the statistical theory of turbulent mixing with chemical reaction, the reader is referred to an article by Corrsin.[1] O'Brien[2] has investigated the statistical behavior of the reactant of a first-order irreversible reaction in isotropic turbulence by using the zero fourth-cumulant approximation. However, the numerical computation shows that the approximation leads to negative concentration spectrum functions.[3] Corrsin[4,5] has obtained

Presented as Preprint 64-19 at the AIAA Aerospace Sciences Meeting, New York, January 20–22, 1964; revision received May 18, 1964. A portion of this work was done at the Department of Mechanics, The Johns Hopkins University, Baltimore, Md.; the research project there was supported by the Fluid Dynamics Branch of the Office of Naval Research. Subsequent work was done at the Boeing Scientific Research Laboratories. The author wishes to express his gratitude to Stanley Corrsin for suggesting this problem and for subsequent discussions, suggestions, and comments. He is also indebted to M. E. Graham and F. H. Champagne for reading the manuscript and to W. C. Cook for the numerical computations.

* Staff Member, Aerodynamics and Propulsion Group, Flight Sciences Laboratory. Member AIAA.